JOURNAL OF OPTOELECTRONICS AND ADVANCED MATERIALS Vol. 9, No. 3, March 2007, p. 527 - 531

Magnetic nanoparticles for biomedical applications

M. FARDIS*, I. RABIAS, G. DIAMANTOPOULOS, N. BOUKOS, D. TSITOURLI, G. PAPAVASSILIOU, D. NIARCHOS

Institute of Materials Science, National Centre for Scientific Research 'Demokritos', 153 10 Aghia Paraskevi, Athens, Greece

Magnetite nanoparticles covalently coated with polysaccharide arabic acid are investigated as possible constituents of aqueous ferrofluids for biomedical applications. The nanoparticles have been characterized by transmission electron microscopy and with magnetic measurements. ^{1}H nuclear magnetic resonance T_1 relaxation experiments of the coating which cover the nanoparticles have been also carried out in an attempt to probe the dynamic (superparamagnetic) behaviour of the magnetic nanoparticles. Finally, magnetic hyperthermia experiments of the synthesized ferrofluid have been performed and the dependence of the measured Specific Absorption Rate coefficient (SAR) as a function of the amplitude of the irradiation field is discussed.

(Received November 15, 2006; accepted December 21, 2006)

Keywords: Ferrofluids, Magnetic nanoparticles, NMR, Magnetic hyperthermia

1. Introduction

Magnetic fluids or ferrofluids are stable colloidal suspensions of ultra-fine particles of a ferromagnet or ferrite in any ordinary liquid (e.g. water, liquid hydrocarbon, etc.) [1]. The dimensions of the ultra-fine particles lie in the nanometer scale (hence the term magnetic nanoparticles is also encountered) and for magnetite - the most popular ferrite material to prepare magnetic fluids, it is found that for stable colloids which do not coagulate and aggregate, the diameters of the particles must be less than around 15 nm [1]. A popular synthetic method in order to prevent agglomeration is the coating of the nanoparticles with appropriate non-magnetic materials. The colloidal suspensions of coated magnetic nanoparticles have been recently the focus of intensive research not only for the study of the physics of magnetism in the nanometer scale [2], but also for the use of ferrofluids in many technological and biomedical applications such as technical heating processes, media contrast agents in Magnetic Resonance Imaging (MRI) and as therapeutic agents for RF-magnetic hyperthermia [3, 4, 5].

2. Experimental

An iron oxide (Fe_3O_4) based ferrofluid with arabic acid polysaccharide coating was synthesized by the reaction of ferric chloride and ferrous chloride in the presence of ammonia, using a new route in coprecipitation method. The nominal molecular weight of the arabic acid used was 250,000. Dry powders of the coated magnetic nanoparticles were then prepared and subsequently characterized by a number of techniques including Transmission Electron Microscopy (Philips CM20, TEM), X-ray diffraction, VSM and SQUID (MPMSR2) magnetometry and Nuclear Magnetic Resonance spectroscopy.

^{1}H pulsed Nuclear Magnetic Resonance experiments as a function of temperature were performed at 2.35 Tesla using a conventional coherent NMR spectrometer. An Oxford 1200 CF continuous flow cryostat was employed for measurements in the range 77-300 K. T_1 spin-lattice relaxation time was measured using the saturation recovery spin-echo pulse sequence.

Magnetic hyperthermia experiments were performed using an induction heating furnace equipped with water cooled coils, operating at a fixed frequency of 380 kHz and delivered a maximum output power of 15 kW. The amplitude of the induced radiofrequency field was measured by monitoring the inductive root mean square value of voltage (Vrms) at a coil placed inside the water cooled coil.

3. Results and discussion

TEM Microscopy

A typical TEM bright field image of the arabic acid coated ferrofluid sample is shown in Fig. 1. From the analysis of the TEM images of the sample, the core size of the nanoparticles is ranging from 7 to 10 nm.

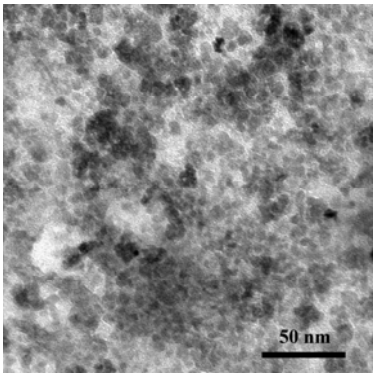

Fig. 1. TEM image of arabic acid coated ferrofluid.

Magnetization measurements

The macroscopic magnetic moment of the coated magnetic nanoparticles was measured at room temperature as a function of the magnetic field using a vibrating sample magnetometer with the applied field varying between ± 20 kOe. The magnetization data for the arabic acid coated nanoparticles are shown in Fig. 2.

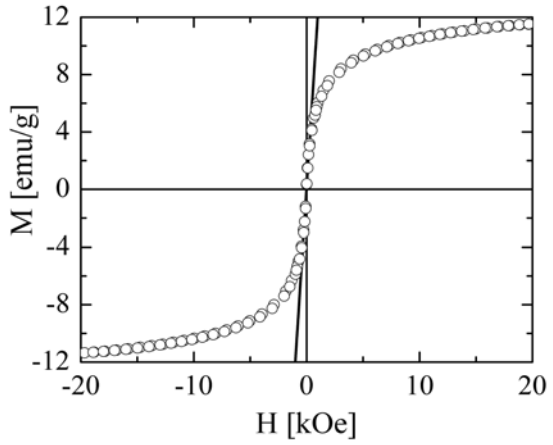

Fig. 2. Magnetization for dry powder sample of coated nanoparticles. The line is a linear fit to the low field data near the origin.

Assuming that the sample consists of non-interacting, single-domain particles in the superparamagnetic state, the magnetization is described by the Langevin function [6]:

$$L\left(\frac{\mu H}{k_B T}\right) = \coth\left(\frac{\mu H}{k_B T}\right) - \frac{\mu H}{k_B T} \qquad (1)$$

where μ is the magnetic moment of a particle, H is the applied field and k_B is the Boltzmann constant. Since inevitably there will be a distribution of the sizes of the magnetic particles, it is a custom practice [7] to introduce a distribution function of the magnetic moments $f(\mu)$ and the magnetization $M(H, T)$ is then described by:

$$M(H,T) = \int_0^\infty \mu L\left(\frac{\mu H}{k_B T}\right) f(\mu) d\mu \qquad (2)$$

The saturation magnetization M_s is given by [7]:

$$M_s = \int_0^\infty \mu f(\mu) d\mu = N < \mu > \qquad (3)$$

where $<\mu>$ is the mean magnetic moment per particle and N is the number of particles per unit volume of the sample.

For the distribution $f(\mu,)$ a lognormal distribution of magnetic moments is frequently employed [7],

$$f(\mu) = \frac{N}{\sqrt{2\pi}\sigma}\frac{1}{\mu}\exp\left[-\frac{\ln^2\left(\mu/\mu_0\right)}{2\sigma^2}\right] \qquad (4)$$

where μ_0 and σ are the median and the width of the distribution respectively.

The moments of the lognormal distribution are given by:

$$< \mu^q >= \mu_0^q \exp\left(q^2\sigma^2/2\right) \qquad (5)$$

Therefore, the mean magnetic moment <μ> is given by: $<\mu> = \mu_0 \exp(\sigma^2/2)$ [7].

For the analysis of the data we use the low and the high field region of the magnetization curve as follows:

For high fields, $\mu H/k_B T >> 1$ and therefore $L(\mu H/k_B T) \approx 1 - k_B T/\mu H$. In this case the magnetization near saturation is given by [7]:

$$M = N < \mu > \left(1 - \frac{k_B T}{< \mu > H}\right) \qquad (6)$$

The magnetization data plotted according to Eq. (6) i.e. M as a function of $1/H$ are shown in Fig. 3. The saturation magnetization $M_s = N<\mu>$ thus obtained was found to be M_s=12.6 emu/gr much lower than the corresponding one for the bulk magnetite (50 emu/gr), a reduction frequently encountered in the literature [2]. Reduced magnetization in small ferrite particles is well documented in the literature, but the nature of the spin structure in such particles has not been well understood [2]. Proposed mechanisms for moment reduction include shell-core structures, spin canting, spin-glass behaviour etc. [2, 8].

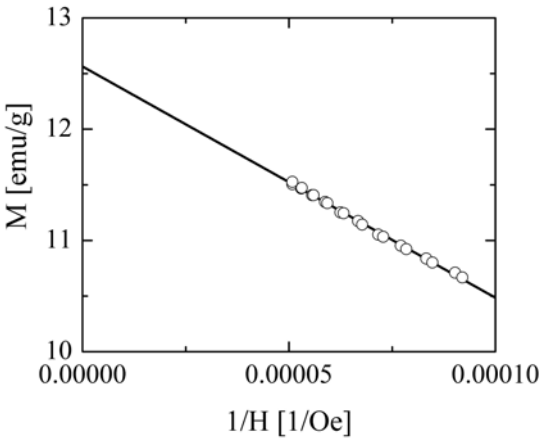

Fig. 3. Magnetization data near saturation, as a function of 1/H. The line is a linear fit to the data.

For low fields $\mu H/k_B T << 1$ and therefore $L(\mu H/k_B T) \approx \mu H/3k_B T$. Thus the magnetization near the origin of the axes in Fig. 2 is given by:

$$M = \frac{H}{3k_B T} N < \mu^2 > \qquad (6)$$

Using the initial slope of the magnetization data in Fig. 2, the saturation magnetization and the moments of the lognormal distribution function as given by Eq. (5), the following statistical parameters for the magnetization are obtained: μ_0=1239 μ_B, $<\mu>$=2707 μ_B, σ=1.25, and N=5.02 10^{17} /g.

The mean magnetic moment $<\mu>=2707\ \mu_B$ corresponds to a mean particle diameter $<d>_{magn}= 4.6$ nm, if I_s = 500 emu/cm^3 is assumed for the saturation magnetization of bulk magnetite [8]. This magnetically derived mean particle diameter $<d>_{magn}= 4.6$ nm, is somewhat smaller than the one (7-10 nm) derived from TEM images (Fig. 1.). This difference is frequently encountered in the literature and may be due to the presence of a magnetic dead layer around the particle, resulting in a magnetic particle volume derived from magnetization data smaller than the crystalline core volume [3].

The temperature dependence of the powder dc magnetic susceptibility of the coated nanoparticles in 10 and 100 Oe is shown in Fig. 4. The lower curve both in 10 and 100 Oe was obtained by cooling the system in zero magnetic fields (ZFC) from 300 K to 4.2 K. The magnetic field H was then applied and magnetization was measured as temperature was increased. The upper curve both in 10 and 100 Oe was obtained by cooling the system but now in the measuring field (FC).

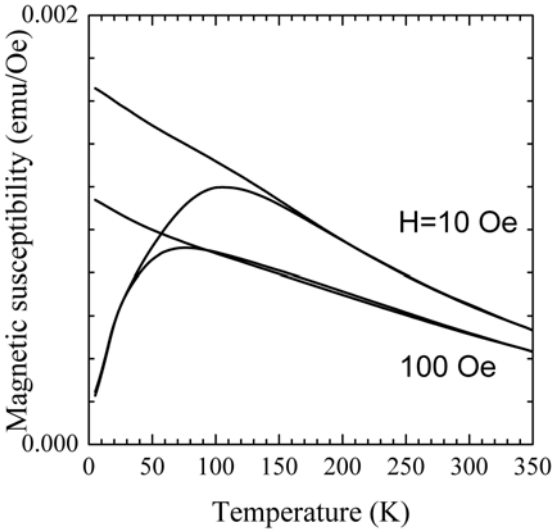

Fig. 4. Magnetic susceptibility χ as a function of temperature, obtained in FC and ZFC modes of dry powder sample of coated nanoparticles at H = 10 and 100 Oe.

The maximum of the ZFC curve is observed at around 80 K and 110 K for H=100 and 10 Oe respectively and is related to the blocking temperature (T_B) of superparamagnetic particles [1]. If a particle has a uniaxial anisotropy characterized by an anisotropy constant K, then the direction of the magnetic moment is confined to the direction of the easy axis of the particle. With the increase in the temperature T the thermal energy k_BT overcomes the barriers of the magnetic anisotropy energy $K\upsilon$, where υ is the particle volume. As the temperature is lowered, the thermal fluctuations reduce and the continuous tumbling of the moments are gradually replaced by 180^0 moment flips between the two easy directions. With decreasing temperature, the time between these superparamagnetic reversals increases until it is comparable to the measuring time of an experiment. Below this temperature, T_B, the moment will appear to be stationary, or blocked [9]. The shift of the peak with the applied field is due to an increased blocking temperature due to enhanced energy barriers. The FC and ZFC branches merge each other at higher temperatures for H=100 Oe at around 90 K and for 10 Oe at 160 K. This reversible behaviour for $T>T_B$ suggests minor contributions from larger particles to the unblocking process. The application of an external field apparently increases the barriers to spin reorientation. For a larger field, H=1000 Oe one could expect the magnetic energy to dominate the interaction energy.

NMR relaxation measurements

In order to probe the dynamic behaviour of the superparamagnetic nanoparticles using nuclear magnetic resonance techniques the following experiment was carried out. We observed the NMR signal of the protons (^{1}H) contained in the coating of the nanoparticles as a function of temperature. In particular we measured the ^{1}H spin-lattice relaxation time T_1 of arabic acid in (a) arabic acid coated magnetic nanoparticles and (b) arabic acid powder alone for comparison reasons. The measurements were performed at an applied field of 2.4 Tesla (which correspond to an NMR Larmor frequency of 100 MHz) between room and liquid-nitrogen temperatures. The T_1 relaxation data as a function of temperature are shown in Fig. 5.

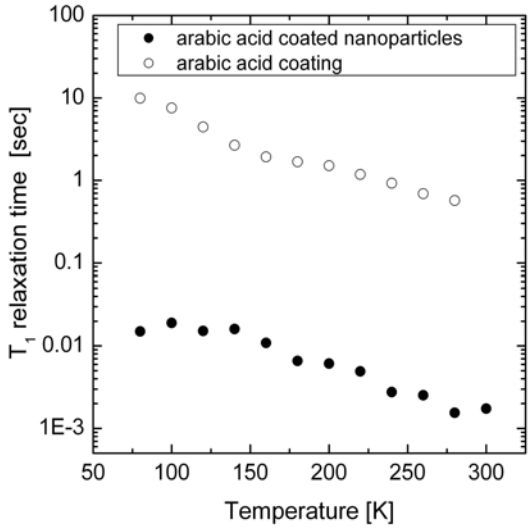

Fig. 5. ^{1}H T_1 spin-lattice relaxation time of arabic acid as a function of temperature in (a) arabic acid coated nanoparticles (filled circles) and (b) powder arabic acid (open cir circles).

It is observed that the T_1 relaxation time for the coated nanoparticles is three orders of magnitude lower than the T_1 of the bulk powder thus ensuring that the protons in the coated nanoparticles are directly influenced by the Fe_3O_4 magnetic moments through the electron-nucleus dipolar interaction. What is surprising is that the general behaviour of the temperature dependence of T_1 relaxation is the same for the coated

nanoparticles (filled circles in Fig. 5) and for the coating itself (open circles in Fig. 5) which is a diamagnetic material.

In the high temperature range of the relaxation data an activated behaviour is present as is shown in Fig. 6, where the relaxation rate $1/T_1$ is plotted as a function of the inverse temperature $1/T$.

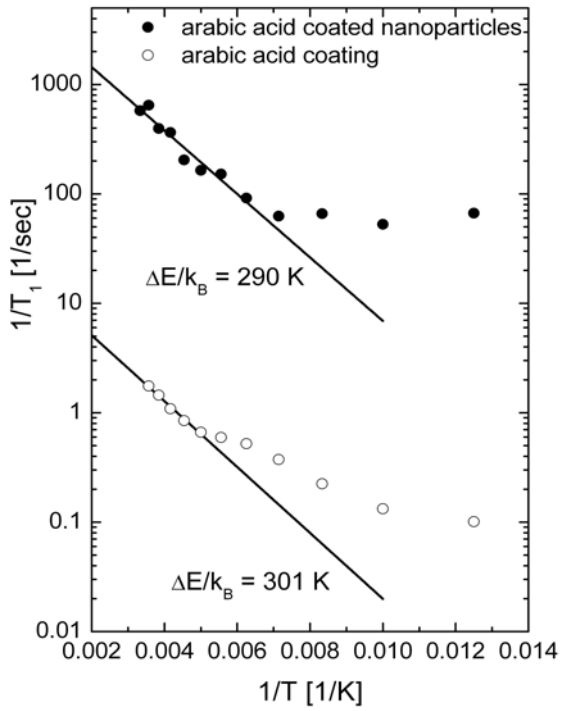

Fig. 6. $1/T_1$ relaxation rate as a function of inverse temperature 1/T for (a) arabic acid coated nanoparticles (filled circles) and (b) arabic acid coating (open cir circles). The solid lines are fits to the Arrhenious law given by Eq. (7).

The activation mechanism can be described by an Arrhenious expression of the form:

$$\frac{1}{T_1} = \left(\frac{1}{T_1}\right)_0 \exp\left(-\frac{\Delta E}{k_B T}\right) \qquad (7)$$

where ΔE is the activation energy.

The fits of Eq. (7) in the relaxation data in Fig. 6 in the high temperature range are shown as solid lines and yield $\Delta E/k_B$ = 290 and 301 K for the coated nanoparticles and the coating alone respectively. It is observed that the calculated activation energies for the two samples are nearly the same and indicate the significance of the thermal fluctuations of the magnetic moments in the coated nanoparticles. If the activation energy ΔE is identified with the activation energy associated with the magnetic anisotropy energy $K\upsilon$, then a particle volume υ = 200 nm^3 is calculated for the coated nanoparticles, using K = 2x10^5 erg/cm^3, the magnetocrystalline anisotropy constant of bulk magnetite. The particle diameter corresponding to the above volume υ, is 7.2 nm which is well correlated with the mean diameter from the magnetization measurements of 4.6 nm, and the ones from the TEM images, considering the approximations involved and particularly the fact that the NMR measurements were performed at the high field of 2.4 Tesla where most of the magnetic moments are aligned along the field direction.

Magnetic hyperthermia experiments

A promising application of magnetic fluids in the field of nanomedicine is heating by radiofrequency (RF) induction [10]. This method involves irradiation of the magnetic fluids with an alternating electromagnetic field (AC) and absorption of the energy of the AC field. The energy is then transformed to heat by several physical mechanisms like hysteresis losses, relaxation losses and resonance losses [11]. The efficiency of this transformation depends on several parameters like the size of the particles, the frequency of the AC field, the field amplitude, the coating, the nature and shape of the particles and so on. The efficiency of the transformation is measured by the specific power absorption rate (SAR), measured in watts per gram of magnetic material and given by the following equation [12]:

$$SAR = \frac{W}{m_{Fe}} = \frac{\Delta Q}{\Delta t m_{Fe}} = c\frac{m_f}{m_{Fe}}\frac{\Delta T}{\Delta t}, \text{ in W/g}_{\text{Fe}} \qquad (8)$$

where c is the specific heat capacity of the ferrofluid, calculated as the mass weighted mean value of magnetite and water, m_f is the mass of the ferrofluid, and m_{Fe} is the mass of the iron in the ferrofluid.

Measurement of the heating rate $\Delta T/\Delta t$ were performed for the ferrofluid suspension of the arabic acid coated nanoparticles and the SAR values as a function of the amplitude H of the alternating irradiation field (AC) are shown in Fig. 7.

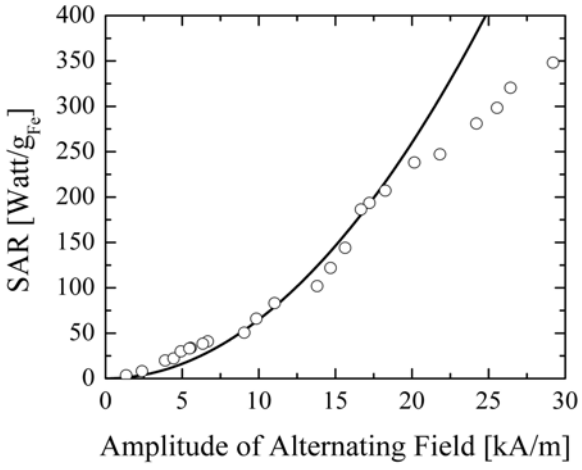

Fig. 7. Specific Absorption Rate (SAR) of arabic acid coated nanoparticles as a function of the amplitude of the irradiation field H. The solid line indicates the square law dependence: SAR~H^2.

The dependence of the SAR coefficient with the amplitude of the alternating field has not thoroughly investigated for high field values. It has been established that for nanoparticles exhibiting superparamagnetic behaviour, the SAR coefficient depends on the square of the AC field, according to the relation [4, 13]:

$$SAR = \mu_0 \pi \chi'' f H^2 \quad (9)$$

where μ_0 is the permeability of free space, χ'' is the imaginary part of the complex dynamic susceptibility and f is the frequency.

It is evident in Fig. 7, that the SAR coefficient is proportional to H^2 for low AC field values as shown by the solid line which indicates the square law dependence. However, for high AC field values a departure from the above dependence and a rather linear relation SAR~H is observed, above around 15 kA/m (190 Gauss).

This behaviour is probably attributed to the onset of non-linear dependence between the magnetization and the applied AC field for high field amplitudes [14]. This is due to the fact that an increase in field strength without limit cannot lead to a similar increase in magnetization, as shown by the numerical calculations of the dynamic susceptibility in Ref. 14.

4. Conclusions

The magnetic properties of magnetite nanoparticles covalently coated with polysaccharide arabic acid were investigated in order to access their effectiveness of the associated ferrofluids in biomedical applications. The TEM and magnetic measurements showed that the particles exhibited a superparamagnetic behaviour as expected for nanometer particles with a magnetic core diameter of around 5 nm. The NMR relaxation experiments provided the activation energy for the fluctuations of the magnetic moments. Finally, the high SAR values obtained in magnetic hyperthermia experiments on the aqueous ferrofluid with the arabic acid coated nanoparticles demonstrated that this ferrofluid could be used for heating applications in biomedicine.

References

[1] J. L. Dormann, D. Fiorani, E. Tronc, Adv. Chem. Phys. **98**, 283 (1997).
[2] R. H. Kodama, J. Magn. Magn. Mater. **200**, 359 (1999).
[3] R. Hergt, R. Hiergeist, M. Zeisberger, G. Glöckl, W. Weitschies, L. P. Ramirez, I. Hilger, W. A. Kaiser, J. Magn. Magn. Mater. **280**, 358 (2004).
[4] R. E. Rosensweig, J. Magn. Magn. Mater. **252**, 370 (2002).
[5] M. Shinkai, J. Biosc. Bioeng. **94**, 606 (2002).
[6] B. D. Cullity, in 'Introduction to Magnetic Materials' Assison-Wesley, Reading, MA, 1972.
[7] E. F. Ferrari, F. C. S. da Silva, M. Knobel, Phys. Rev. B **56**, 6086 (1997).
[8] E. Lima Jr., A. L. Brandl, A. D. Arelao, G. F. Goya, cond-mat/0505683 and references threrein.
[9] J. van Lierop, D. H. Ryan, Phys. Rev. Lett. **85**, 3021 (2000).
[10] A. Jordan, R. Scholz, K. H. Maier, M. Johannsen, P. Wust, J. Nadobny, H. Schirra, H. Schmidt, S. Deger, S. Loening, W. Lanksch, R. Felix, J. Magn. Magn. Mater. **225**, 118 (2001).
[11] R. Hergt, R. Hiergeist, I. Hilger, W. A. Kaiser, Y. Lapatnikov, S. Margel, U. Richter, J. Magn. Magn. Mater. **270**, 345 (2004).
[12] M. Ma, Y. Wu, J. Zhou, Y. Sun, Y. Zhang, N. Gu, J. Magn. Magn. Mater. **268**, 33 (2004).
[13] D. C. F. Chan, D. B. Kirpotin, P. A. Bunn Jr., J. Magn. Magn. Mater. **122**, 374 (1993).
[14] A. Yu. Zubarev, A. V. Yushkov, JETP **87**, 484 (1998).

*Corresponding author: mfardis@ims.demokritos.gr